

Torque control strategy for fault –tolerant “five-phase PMSG-PWM rectifier” set for marine current turbine applications

A. Dieng¹, J.C. Le Claire², M.F. Benkhoris², M. Ait-Ahmed²

Université Cheikh Anta Diop de Dakar – Ecole Supérieure Polytechnique de Dakar¹

IREENA – UNIVERSITY OF NANTES²

Laboratoire LER¹

37 boulevard de l'université – BP406 – 44602 Saint-Nazaire Cedex, France²

Tel : 00 221 776665138¹, (+33)2 40 17 26 02²

E-Mail: abdoulaye.dieng@esp.sn¹, jean-claude.le-claire@univ-nantes.fr², mohamed-fouad.benkhoris@univ-nantes.fr², mourad.ait-ahmed@univ-nantes.fr²

Abstract—This paper deals Torque control strategy for fault – tolerant “five-phase PMSG-PWM rectifier” set for marine current turbine applications. Based on Fortescue transformation a dynamical model of “five phase PMSG non sinusoidal EMF” in natural basis is established. In order to maximize the average torque, to minimize the copper losses and to reduce the torque ripples all harmonics of EMF are exploited not only for the normal operation mode but also under open phase conditions. Thus, an adequate stator phase current waveforms are synthesized in natural basis (abcde). To ensure an effective tracking of these currents waveforms a robust nonlinear model-free controller with a large bandwidth is proposed. Simulation and experimental results highlight the performances of the control strategy and confirm the efficiency and the robustness of the proposed controller.

Index Terms— Five-Phase PMSG, Current Control, AC current controller, Fault tolerant control, Torque control strategy

I. INTRODUCTION

Multiphase permanent magnet synchronous generator (PMSG) seems to be an attractive solution in the context of renewable energy source exploitation and in case of fault tolerant applications [1], [2]. The association of multiphase PMSG to AC-DC converter increases the converted power, segments the electrical power and ensures the energy conversion chain under fault operation. This paper deals with an improved torque control strategy for fault –tolerant “five-phase PMSG-PWM rectifier” set for marine current turbine applications. All currents harmonics and EMF harmonics which contribute positively to the torque are exploited. In the literature, many papers deal with MCT applications or Wind

turbine applications and the proposed control strategy is done in the dq Park frame because the dq current references are constants and a simple PI controller is sufficient for a good control. Nevertheless, in the case of open-circuit failure due to the failure of a power active component of the rectifier, the machine can still continue to operate using the remaining healthy phases but a torque ripples appear. The torque control strategy need to impose a new optimal current references in order to reduce the torque ripples and minimize the copper losses. Many methods are proposed in order to determinate these current references [3]-[10]. A vectorial approach in real time is proposed in [10]. Another method using the Lagrangian approach via optimization is used in [8], [9]. In our paper an optimal current references are obtained via the model of the five-phase PMSG - AC/DC rectifier set under fault operation. The same strategy under normal operation is adopted. Nevertheless these current references are not constants in the dq frame or neither in the abcde frame as highlighted in [10]-[18]. Then an accurate and robust controller is requested as proposed in [10]-[18]. As the new current references are not constants in the dq frames, it is not necessary to develop a dynamical model in view of control of the 5-phase PMSG in the Park frame. An adequate model in the abcde frame or Concordia's frame is sufficient. In all cases robust controller which has a large bandwidth is needed. Many controllers are investigated and proposed in the literature. In [15], [16] a fractional controller is proposed while in [10], [18] a hysteresis regulator is used. In [13] a second-order sliding mode control is proposed and in [17] a H_∞ controller is proposed too. In [11] fuzzy logic and sliding mode controls are used. For the hysteresis regulator the switching frequency of the power device is not controlled. Others methods can be used to control maximum switching frequency of the power

The second subspace is called the secondary frame and it is deduced from the 3rd and 4th columns of $[M_5]$. The first column of $[M_5]$ is the zero sequence. Then, each physical vector $[X]$ (voltage, current, EMF) can be projected in the well subspace according the following complex formulation and taking into account the direct sense:

$$[X]_h = C_h e^{j(h\theta + \varphi_h)} \begin{bmatrix} 1 \\ a^{4h} \\ a^{3h} \\ a^{2h} \\ a^h \end{bmatrix} \quad (3)$$

Where h is the rank of the harmonic, C_h and φ_h are respectively the magnitude and the phase of the harmonic 'h'.

Using (2) and (3), the harmonics repartition of the 5-Phase PMSG is summarized in Table I.

TABLE I
HARMONICS REPARTITION OF THE 5-PHASE PMSG

Subspaces	Main frame	Secondary frame	Homopolar
Harmonic order	1,4,6,9,...	3,2,7,8,...	5,10,15,...

Indexing the direct sense of the main frame on the fundamental and looking the sequence order of the matrix $[M_5]$, the direct sense of the secondary frame is indexed automatically on the third harmonic. Therefore, in the natural abcde frame the Five-Phase PMSG is equivalent to three fictitious Five-Phase PMSG, called respectively main machine where the electrical pulse is ω , secondary machine where the electrical pulse is 3ω and homopolar machine. Fig. 2 illustrates the new fictitious repartition of phases of the main and secondary machines.

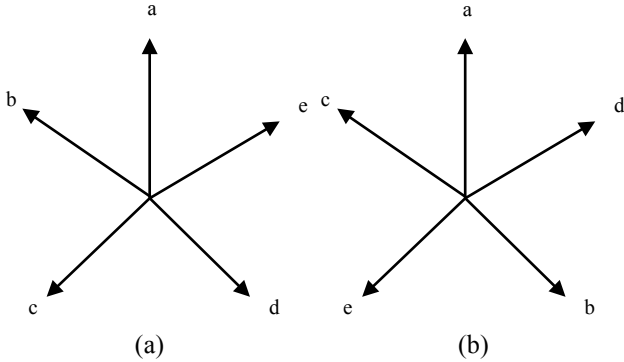


Fig. 2. New fictitious repartition of phases ((a) main machine), ((b) secondary machine)

The harmonics (EMF, current, voltage and flux) which are projected in the main frame will be seen only by the main machine and the harmonics which are projected in the secondary frame will be seen only by the secondary machine. The fifth harmonic and its multiples will be seen by the homopolar machine. Therefore, (1) can be decomposed in the three fictitious frames:

$$[E]_m = [R][I]_m + [L]_m \frac{d}{dt} [I]_m + [V]_m \quad (4)$$

$$[E]_s = [R][I]_s + [L]_s \frac{d}{dt} [I]_s + [V]_s \quad (5)$$

$$[E]_0 = [R][I]_0 + [L]_0 \frac{d}{dt} [I]_0 + [V]_0 \quad (6)$$

Where m, s, h represents respectively the main, secondary and homopolar machine.

Based on the principle of the diagonalization of the matrix inductance $[L]_m, [L]_s$ and $[L]_0$, the electrical equation of each fictitious machine becomes:

$$[E]_y = r[I]_y + L_y \frac{d}{dt} [I]_y + [V]_y \quad y=m,s,h \quad (7)$$

$$L_m = L_1 + 2L_2 \cos\left(\frac{2\pi}{5}\right) + 2L_3 \cos\left(\frac{4\pi}{5}\right)$$

$$L_s = \left[L_1 + 2L_2 \cos\left(\frac{6\pi}{5}\right) + 2L_3 \cos\left(\frac{8\pi}{5}\right) \right]$$

$$L_0 = L_1 + 2L_2 + 2L_3$$

The generator's electromagnetic torque for each fictitious machine is given by:

$$\Gamma_y = \frac{1}{\Omega} (E_{a,y} I_{a,y} + E_{b,y} I_{b,y} + E_{c,y} I_{c,y} + E_{d,y} I_{d,y} + E_{e,y} I_{e,y}) \quad (8)$$

Where $y=m,s,h$

The generator's total electromagnetic torque is given by:

$$\Gamma = \Gamma_m + \Gamma_s \quad (9)$$

It can be shown that the expression (9) is equivalent to the known general expression of the torque given by:

$$\Gamma = \frac{1}{\Omega} (E_a I_a + E_b I_b + E_c I_c + E_d I_d + E_e I_e) \quad (10)$$

Where $E_z = E_{z,m} + E_{z,s}$ and $I_z = I_{z,m} + I_{z,s}$ $z=a,b,c,d,e$

Indeed, as the two sub-machines are decoupled, the sum of the terms due to the interactions between them is equal to zero:

$$\sum_{z=a}^e (E_{z,m} I_{z,s} + E_{z,s} I_{z,m}) = 0 \quad (11)$$

B. Under fault operation

In the case of open-circuit failure corresponding for example to the opening of the fifth phase after failure of a power active component of the rectifier, the voltage equation of the fifth phase, in natural base, becomes:

$$V_e = E_e - \left(L_2 \frac{di'_a}{dt} + L_3 \frac{di'_b}{dt} + L_3 \frac{di'_c}{dt} + L_2 \frac{di'_d}{dt} \right) \quad (12)$$

$$\text{Knowing that } V_a + V_b + V_c + V_d + V_e = 0 \quad (13)$$

It can be shown that:

$$V_{ao} + V_{bo} + V_{co} + V_{do} + V_e = 4V_{No} \quad (14)$$

Where N is the neutral point of the machine

$$\begin{bmatrix} V_a \\ V_b \\ V_c \\ V_d \end{bmatrix} = \begin{bmatrix} V_{ao} - V_{No} \\ V_{bo} - V_{No} \\ V_{co} - V_{No} \\ V_{do} - V_{No} \end{bmatrix} = \frac{1}{4} \begin{bmatrix} 3 & -1 & -1 & -1 \\ -1 & 3 & -1 & -1 \\ -1 & -1 & 3 & -1 \\ -1 & -1 & -1 & 3 \end{bmatrix} \begin{bmatrix} V_{ao} \\ V_{bo} \\ V_{co} \\ V_{do} \end{bmatrix} - \frac{1}{4} V_e \quad (15)$$

By substituting (12) in (15), (15) becomes:

$$\begin{bmatrix} V_a \\ V_b \\ V_c \\ V_d \end{bmatrix} = \begin{bmatrix} V'_a \\ V'_b \\ V'_c \\ V'_d \end{bmatrix} - \frac{1}{4} E_e + L_2 \frac{di'_a}{dt} + L_3 \frac{di'_b}{dt} + L_3 \frac{di'_c}{dt} + L_2 \frac{di'_d}{dt} \quad (16)$$

$$\text{Where: } \begin{bmatrix} V'_a \\ V'_b \\ V'_c \\ V'_d \end{bmatrix} = \frac{1}{4} \begin{bmatrix} 3 & -1 & -1 & -1 \\ -1 & 3 & -1 & -1 \\ -1 & -1 & 3 & -1 \\ -1 & -1 & -1 & 3 \end{bmatrix} \begin{bmatrix} V_{ao} \\ V_{bo} \\ V_{co} \\ V_{do} \end{bmatrix}$$

By substituting (16) in (1), (1) becomes:

$$[E'] = [R'] [I'] + [L'] \frac{d}{dt} [I'] + [V'] \quad (17)$$

$$\text{Where: } [R'] = \begin{bmatrix} r & 0 & 0 & 0 \\ 0 & r & 0 & 0 \\ 0 & 0 & r & 0 \\ 0 & 0 & 0 & r \end{bmatrix}$$

$$[L'] = \begin{bmatrix} L_1 + \frac{1}{4}L_2 & L_2 + \frac{1}{4}L_3 & L_3 + \frac{1}{4}L_3 & L_3 + \frac{1}{4}L_2 \\ L_2 + \frac{1}{4}L_2 & L_1 + \frac{1}{4}L_3 & L_2 + \frac{1}{4}L_3 & L_3 + \frac{1}{4}L_2 \\ L_3 + \frac{1}{4}L_2 & L_2 + \frac{1}{4}L_3 & L_1 + \frac{1}{4}L_3 & L_2 + \frac{1}{4}L_2 \\ L_3 + \frac{1}{4}L_2 & L_3 + \frac{1}{4}L_3 & L_2 + \frac{1}{4}L_3 & L_1 + \frac{1}{4}L_2 \end{bmatrix}$$

It can be noticed that following the open phase, the matrix $[L']$ changes.

The new EMF is:

$$[E'] = \begin{bmatrix} E'_a \\ E'_b \\ E'_c \\ E'_d \end{bmatrix} = \begin{bmatrix} E_a + \frac{1}{4}E_e \\ E_b + \frac{1}{4}E_e \\ E_c + \frac{1}{4}E_e \\ E_d + \frac{1}{4}E_e \end{bmatrix}, [X'] = \begin{bmatrix} X'_a \\ X'_b \\ X'_c \\ X'_d \end{bmatrix} \text{ and } X' = V', I', E'$$

The expression of the total generator's electromagnetic torque is now given by:

$$\Gamma' = \frac{1}{\Omega} (E'_a I'_a + E'_b I'_b + E'_c I'_c + E'_d I'_d) \quad (18)$$

The torque expression can be generalized for any open phase. Therefore the general expression of the matrix $[E']$ can be deduced for any open phase:

$$[E'] = \begin{bmatrix} k_a E'_a \\ k_b E'_b \\ k_c E'_c \\ k_d E'_d \\ k_e E'_e \end{bmatrix} = \begin{bmatrix} k_a \left(E_a - \frac{1}{4}(k_a E_a + k_b E_b + k_c E_c + k_d E_d + k_e E_e) \right) \\ k_b \left(E_b - \frac{1}{4}(k_a E_a + k_b E_b + k_c E_c + k_d E_d + k_e E_e) \right) \\ k_c \left(E_c - \frac{1}{4}(k_a E_a + k_b E_b + k_c E_c + k_d E_d + k_e E_e) \right) \\ k_d \left(E_d - \frac{1}{4}(k_a E_a + k_b E_b + k_c E_c + k_d E_d + k_e E_e) \right) \\ k_e \left(E_e - \frac{1}{4}(k_a E_a + k_b E_b + k_c E_c + k_d E_d + k_e E_e) \right) \end{bmatrix} \quad (19)$$

Where $k_z = 1$ if the corresponding phase is healthy and $k_z = 0$ if the corresponding phase is opened, $z=a,b,c,d,e$.

When $k_z = 0$, the corresponding line from the matrix $[E']$ is removed.

The new expression of the total generator's electromagnetic torque is now given by:

$$\Gamma' = \frac{1}{\Omega} (k_a E'_a I'_a + k_b E'_b I'_b + k_c E'_c I'_c + k_d E'_d I'_d + k_e E'_e I'_e) \quad (20)$$

III. CONTROL STRATEGY OF THE 5-PHASE PMSG

A. Under normal operation

The MPPT strategy is applied. The maximum power available from the tidal current is transformed and injected to the grid. The power transfer is optimal when the losses are minimal. In this case an optimal control strategy that minimizes the reactive power and the copper losses is proposed.

The generator's electromagnetic power is given by:

$$P = P_m + P_s \quad (21)$$

Where $P_m = [E]_m^t [I]_m = \Gamma_m \Omega$ and $P_s = [E]_s^t [I]_s = \Gamma_s \Omega$

The reactive power is equal to zero when the EMF and current vectors of the machine are collinear:

$$\frac{E_{a,i}}{I_{a,i\text{ref}}} = \frac{E_{b,i}}{I_{b,i\text{ref}}} = \dots = \frac{E_{e,i}}{I_{e,i\text{ref}}}, \quad \frac{E_{z,m}}{I_{z,m\text{ref}}} = \frac{E_{z,s}}{I_{z,s\text{ref}}} \quad (22)$$

Where $z = a, b, c, d, e$ and $i = m, s$.

The optimal current references for each fictitious machine in the main and secondary frame can be written:

$$I_{z,i\text{ref}} = \frac{E_{z,i}}{\sum_{z=a}^e E_{z,i}^2} \Gamma_{\text{ref},i} \Omega \quad (23)$$

The total optimal current reference for each phase becomes:

$$I_{z\text{ref}} = \frac{E_z}{\sum_{z=a}^e E_z^2} \Gamma_{\text{ref}} \Omega \quad (24)$$

B. Under fault operation

The same strategy as under normal operation is adopted. Assuming the fifth phase is open-circuited due to the failure of power devices, torque ripples appear.

In order to reduce the torque ripples and to minimize the copper losses, the chosen torque control strategy consists to impose optimal current references in the remaining four phases.

The reactive power is equal to zero when the EMF and current vectors of the machine are collinear:

$$\frac{E'_a}{I'_{a\text{ref}}} = \frac{E'_b}{I'_{b\text{ref}}} = \dots = \frac{E'_d}{I'_{d\text{ref}}} \quad (25)$$

The new optimal current reference for each phase becomes:

$$I'_{z\text{ref}} = \frac{E'_z}{\sum_{z=a}^d E'_z^2} \Gamma'_{\text{ref}} \Omega \quad (26)$$

Where $z = a, b, c, d$.

IV. GENERATION OF THE CURRENT REFERENCES OF THE STUDIED MACHINE

The Fourier analysis of the EMF of the machine under consideration is summarized in Table II. Table II summarizes the normalized magnitude of each harmonic of the considered machine. The fundamental and the ninth harmonics project in the main machine, the third and seventh harmonic in the secondary machine.

TABLE II
FOURIER ANALYSIS OF THE EMF PROFILE

(a) Main machine

EMF Harmonic	1	9
Magnitude/Fundamental %	100%	0.7%

(b) Secondary machine

EMF Harmonic	3	7
Magnitude/Third harmonic %	100%	0.3%

Other harmonics are equal to zero. The ratio of the fundamental and the third harmonic is equal to 30%. It may be noticed that the amplitude of harmonics, particularly the third one, is important and can produce torque.

The Fourier analysis of the EMF shows that the ninth harmonic and the seven harmonic are very low and can be neglected. Then the fundamental and the third harmonic of EMF are only considered. In this case the E_a, E_b, E_c, E_d, E_e expressions are written:

$$[E] = \omega \Phi_m [G(\theta)] + 3\omega \Phi_s [G(3\theta)] \quad (27)$$

Where:

$$[G(\theta)] = \begin{bmatrix} A(\theta) \\ B(\theta) \\ C(\theta) \\ D(\theta) \\ E(\theta) \end{bmatrix} = \begin{bmatrix} \sin(\theta) \\ \sin(\theta - \frac{2\pi}{5}) \\ \sin(\theta - \frac{4\pi}{5}) \\ \sin(\theta - \frac{6\pi}{5}) \\ \sin(\theta - \frac{8\pi}{5}) \end{bmatrix} \text{ and } [G(3\theta)] = \begin{bmatrix} A(3\theta) \\ B(3\theta) \\ C(3\theta) \\ D(3\theta) \\ E(3\theta) \end{bmatrix} = \begin{bmatrix} \sin(3\theta) \\ \sin 3(\theta - \frac{2\pi}{5}) \\ \sin 3(\theta - \frac{4\pi}{5}) \\ \sin 3(\theta - \frac{6\pi}{5}) \\ \sin 3(\theta - \frac{8\pi}{5}) \end{bmatrix}$$

Where Φ_m, Φ_s are respectively the maximum magnitudes of the flux in the main and in the secondary machine, $\omega = p\Omega$ is the electrical angular speed and p is the number of pair poles and it is equal to 3 for the considered machine.

A. Under normal operation

According to (24) and (27) the global optimal current references of the considered machine can be written:

$$[I_{ref}] = \frac{1}{\frac{5}{2}(\omega^2\Phi_m^2 + 9\omega^2\Phi_s^2)} \{\omega\Phi_m[G(\theta)] + 3\omega\Phi_s[G(3\theta)]\} \Gamma_{ref} \Omega \quad (28)$$

Where $[I_{ref}] = [I_{aref} \ I_{bref} \ I_{cref} \ I_{dref} \ I_{eref}]^t$

Let us consider $x = \frac{3\Phi_s}{\Phi_m}$, (28) becomes:

$$[I_{ref}] = \frac{1}{\frac{5}{2}\Phi_m(1+x^2)} \{[G(\theta)] + x[G(3\theta)]\} \Gamma_{ref} \quad (29)$$

$$[I_{ref}] = I_m[G(\theta)] + I_s[G(3\theta)] \quad (30)$$

Where I_m, I_s are respectively the maximum magnitude of the fundamental current (main machine) and the third harmonic current (secondary machine).

$$I_m = \frac{1}{\frac{5}{2}\Phi_m(1+x^2)} \frac{\Gamma_{ref}}{3}, \quad I_s = x I_m, \quad x = \frac{3\Phi_s}{\Phi_m} = 0.3$$

Assuming the phase shift between the measured currents and the current references tends to zero thanks to the AC current controller, the generator's average electromagnetic torque is given by:

$$\Gamma = \Gamma_m + \Gamma_s = \frac{5}{2}(3\Phi_m I_m + 9\Phi_s I_s) \quad (31)$$

As previously mentioned, the adopted strategy allows to minimize the copper losses. Indeed the global copper losses taking into account the contribution of the third harmonic are given by:

$$P_{jm,s} = 5R_s(I_m^2 + I_s^2) \quad (32)$$

For given constant torque the copper losses by exploiting only the main machine can be written:

$$P_{jm} = 5R_s I_m^2 (1 + x^2)^2 \quad (33)$$

The ratio of the two copper losses gives:

$$\frac{P_{jm,s}}{P_{jm}} = \frac{1}{1+x^2} = 92\% \quad (34)$$

The exploitation of the secondary machine, with given torque, reduces the copper losses thus it permits to get an optimal power transfer.

B. Under fault operation

When one phase of the 5-phase PMSG is open-circuited (j^{th} phase), if the same currents under normal operation and their magnitudes are maintained, the expression of the global torque, is given by:

$$\Gamma_d = \Gamma - \frac{1}{\Omega} E_z I_z \quad (35)$$

Where $z = a$ or b or c or d or e according to the open j^{th} phase.

After development, (37) becomes:

$$\Gamma_{d,j} = \frac{4}{5}\Gamma - \frac{1}{2}(T(2\theta) + T(4\theta) + T(6\theta)) \quad (36)$$

Where

$$T(2\theta) = (3\Phi_m I_m + (3\Phi_m I_s + 9\Phi_s I_m)) \cos 2\left(\theta - (j-1)\frac{2\pi}{5}\right)$$

$$T(4\theta) = -(3\Phi_m I_s + 9\Phi_s I_m) \cos 4\left(\theta - (j-1)\frac{2\pi}{5}\right)$$

$$T(6\theta) = 9\Phi_s I_s \cos 6\left(\theta - (j-1)\frac{2\pi}{5}\right)$$

Assuming the fifth phase (corresponding to the phase e) is open-circuited, the expression of the global torque becomes:

$$\Gamma_d = \frac{4}{5}\Gamma - \frac{1}{2}\left\{(3\Phi_m I_m + (3\Phi_m I_s + 9\Phi_s I_m)) \cos 2\left(\theta - \frac{8\pi}{5}\right) - (3\Phi_m I_s + 9\Phi_s I_m) \cos 4\left(\theta - \frac{8\pi}{5}\right) + 9\Phi_s I_s \cos 6\left(\theta - \frac{8\pi}{5}\right)\right\} \quad (37)$$

When the same currents under normal operation and their magnitudes are maintained the generator torque is pulsating and the average value decrease (Fig. 3). The ratio between the torque ripples and the average value of the generator torque is around 60%.

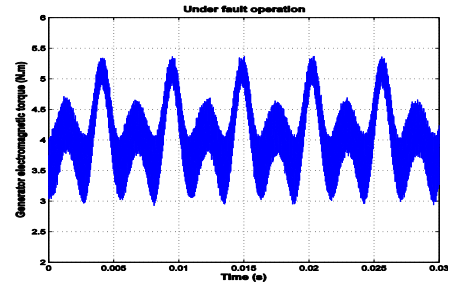


Fig. 3. Electromagnetic torque under fault operation

Now in order to reduce the torque ripples and to minimize the copper losses, the new current references given by (26) are imposed.

Under fault operation, assuming the fifth phase is open-circuited, the new E'_a, E'_b, E'_c, E'_d expressions, determined in the subsection II-B, are deduced:

$$\begin{bmatrix} E'_a \\ E'_b \\ E'_c \\ E'_d \end{bmatrix} = \omega\Phi_m \left\{ \begin{bmatrix} A(\theta) \\ B(\theta) \\ C(\theta) \\ D(\theta) \end{bmatrix} + \frac{1}{4}E(\theta) \right\} + 3\omega\Phi_s \left\{ \begin{bmatrix} A(3\theta) \\ B(3\theta) \\ C(3\theta) \\ D(3\theta) \end{bmatrix} + \frac{1}{4}E(3\theta) \right\} \quad (38)$$

By replacing the E'_a, E'_b, E'_c, E'_d expressions in (26), the global optimal current references of the considered machine under fault operation are obtained:

$$[I'_{ref}] = \frac{1}{F(\theta)} \left\{ \Phi_m \left\{ [G'(\theta)] + \frac{1}{4}E(\theta) \right\} + 3\Phi_s \left\{ [G'(3\theta)] + \frac{1}{4}E(3\theta) \right\} \right\} \Gamma_{ref} \quad (39)$$

$$\text{Where } [G'(\theta)] = \begin{bmatrix} A(\theta) \\ B(\theta) \\ C(\theta) \\ D(\theta) \end{bmatrix} \text{ and } [G'(3\theta)] = \begin{bmatrix} A(3\theta) \\ B(3\theta) \\ C(3\theta) \\ D(3\theta) \end{bmatrix}$$

$$[I'_{ref}] = [I'_{aref} \ I'_{bref} \ I'_{cref} \ I'_{dref}]^t$$

$$F(\theta) = \frac{15}{2}\Phi_m^2(1+x^2) - \frac{15}{4}\left(\Phi_m \sin\left(\theta - \frac{8\pi}{5}\right) + 3\Phi_s \sin 3\left(\theta - \frac{8\pi}{5}\right)\right)^2$$

V. AC CURRENT CONTROLLER

Controllers such as Hysteresis Self-Oscillating (HSO) and Phase-Shift Self-Oscillating (PSSO) are able to achieve high performances. They are robust [25] and are used in many application areas such as Class-D audio amplifiers where low output impedance, extremely low voltage levels of distortion and simple implementations with analog devices are requested [26]. So, relay feedback controls without hysteresis such as PSSO controls are very efficient and then in this work each of the current controls involve a PSSO controller that has been used in DC/AC converters [21] and AC/DC converters [19]. It

has been patented [20]. Its concept combines two ideas. This controller must act at lower frequencies for current regulation and it must act at higher frequencies for switching frequency control. In such way, an analog filter is added in the feedback loop in order to induce a phase-shift, which causes a self-oscillation. This is the reason why it is a PSSO PWM controller. Fig. 4 shows one of its basic schemes where the inverter delivers the output voltage $u(t)$ to an inductive load and the current sensor (whose transfer equals R_T) is used to create a current to voltage feedback.

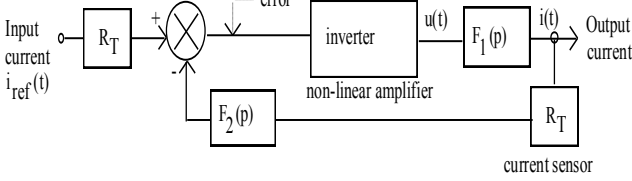


Fig. 4. Scheme of the inverter current control loop

The state of the inverter depends on the error $\varepsilon(t)$. If $\varepsilon(t)$ is positive, $u(t)$ is positive. If $\varepsilon(t)$ is negative, $u(t)$ is negative. A sign block may be drawn on the figure, but this is not done in order to simplify. It should be shown between the error detector and the inverter input. Here, the F_2 's filter is added in order to cause and control the self-oscillation and then the switching frequency of the power devices. The transfer functions $F_1(p)$, $F_2(p)$ and R_T respectively depict the load voltage to current transfer function, the second order low-pass filter transfer function and the current sensor transfer one. They are given by:

$$F_1(p) = \frac{I(p)}{U(p)} = \frac{1}{R + Lp} = \frac{1}{R} \cdot \frac{1}{1 + \frac{L}{R}p} \quad (40)$$

$$F_2(p) = \frac{1}{1 + 2\frac{p}{\omega_0} + \frac{p^2}{\omega_0^2}} \quad (41)$$

Where L is the load's inductance, r the load's resistance, ξ is the damping factor of the second order low-pass filter and ω_0 is its natural frequency.

Thus, it is possible to determine the transfer function $H(p)$ that relates to the linear part of the system without the error detector. It takes into account $F_1(p)$, R_T and $F_2(p)$. Thanks to $H(p)$, the system oscillates at the switching frequency where the total phase shift becomes 0° modulo 360° (with the error detector) and the oscillation frequency is found by requiring that the argument of $H(p)$ equals -180° [27]. In details, thanks to this third order low-pass transfer function $H(p)$, the phase-shift can rotate from 0° to -270° and then the system gives birth to a self-oscillation and the amplifier oscillates at the frequency where the feedback network has a 180 degrees phase-shift and the non-linear amplifier adjusts itself for unity loop gain at the switching frequency [28]. This can be written as the conditions of Heinrich Georg Barkhausen concerning oscillators. Taking into account a reference which equals zero, the conditions of Barkhausen permit to get the oscillation frequency f_{osc} (assuming the $H(j\omega)$'s imaginary part equals zero) and the gain of the amplifier gain A_0 at this frequency (assuming the $-H_{CC}(j\omega)$'s real part equals unity). Then the oscillation frequency f_{osc} comes [21]:

$$\frac{f_{osc}}{f_0} = \frac{osc}{0} = \sqrt{1 + \frac{2}{0.1}} = \sqrt{1 + 2} \cdot \frac{f_{cl}}{f_0} \quad (42)$$

It depends of the load's time constant τ_l multiplied by the

natural frequency f_0 of the F_2 's filter. By comparing the F_1 's cut-off frequency f_{cl} with the F_2 's natural frequency f_0 , it can be observed that f_{osc} depends on the F_2 's filter and is slightly sensitive to the F_1 's parameters. Thus the F_2 's filter controls the switching frequency of the inverter [21]. In fact the oscillation frequency previously defined is the maximum switching frequency. It is possible to find its instantaneous value using Boiko's works [29]. Another tool presented in [30] could be used in order to do it.

VI. RESULTS

This work focuses on the current control performances of the five-phase PMSG. For the marine current turbine simulator the control strategy developed in [22] and the model proposed in [23] are used. Simulations are carried out using Matlab Simulink. The experimental prototype used to validate the proposed control strategy is illustrated by Fig. 5. It involves a 3 kW DC machine, 3kW five-phase PMSG, five-phase PWM rectifier and a 4 quadrant inverter which controls the DC machine in order to emulate the marine turbine. A DSPACE 1103 development board which is interfaced to a standard PC is used to generate the control algorithms. Current measurements are done thanks to sensors LEM LA25-NP. An absolute encoder attached to the generator shaft measures the electrical angular position and the mechanical angular speed of the generator. The DC machine ensures the equivalent speed of the tidal current, the mechanical torque of the turbine and the gearbox. To better show the performance achieved by the inner current control loop it is only interested in an operating point. In this case for the tidal current, assuming that the swell effects are neglected, the speed tidal current is supposed constant. It is true when a period of 60mn is considered. Under fault operation an open-circuit failure is introduced in the fifth phase (phase e). The figures of the generator torque, the generator speed and the generator active power are obtained by using the Control Desk Software. The figures of the currents are obtained by using a scope PM3394.

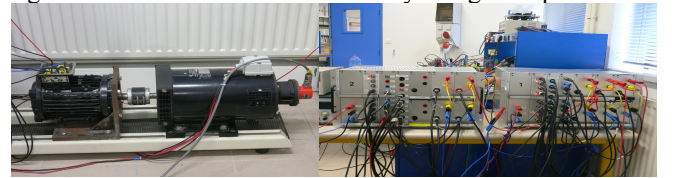


Fig. 5. Part of the experimental bench

A. Under normal operation

Figs. 6 and 7 show the simulated and experimental results. All current references are under control of the chosen AC current controller, where the natural frequency of the filter F_2 equals 18.4 kHz. Then the maximum switching frequency is limited to this value. All simulated results are in accordance with the experimental results. Figs. 6(c), 7(e) and 7(f) show the good performance of the AC current controllers which accurately track its references.

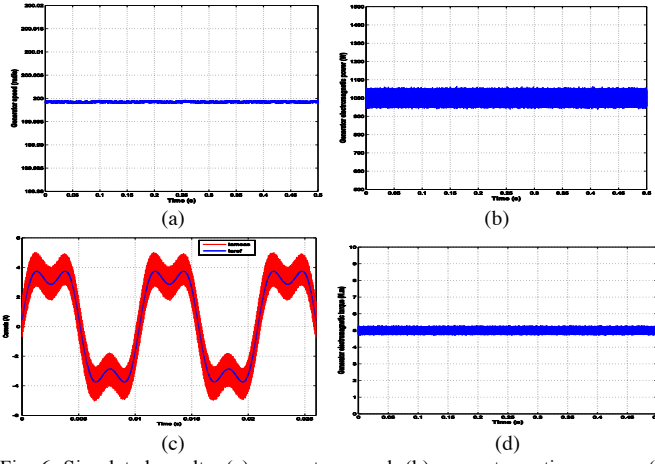


Fig. 6. Simulated results; (a) generator speed, (b) generator active power, (c) currents in the phase a, (d) generator electromagnetic torque

No disturbances have been observed in the generator torque (Fig. 6(d), Fig. 7(c)), the generator speed (Fig. 6(a), Fig. 7(a)), the generator active power (Fig. 6(b), Fig. 7(b)). The proposed control strategy is proved by Figs. 7(d) and 7(e). The phase shift between the EMF (without load) and the current reference is equal to zero (Fig. 7(d)).

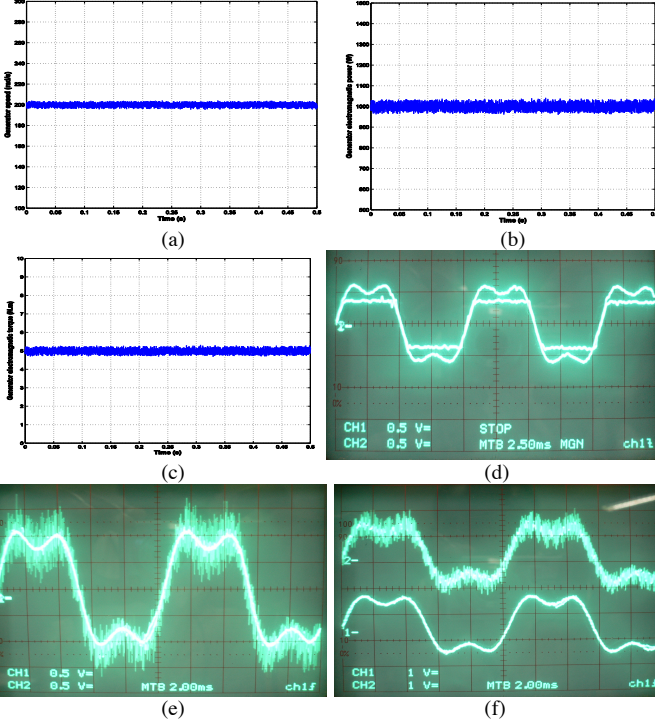


Fig. 7. Experimental results; (a) generator speed, (b) generator active power, (c) generator electromagnetic torque, (d) current reference and EMF in the phase a, (e) and (f) currents in the phase a

As the phase shift between the measured currents and the current references tends to zero (thanks to the AC current controllers which track accurately its references) and the phase shift between the EMF (without load) and the measured current tends to zero too, the power transfer is optimal.

B. Under fault operation

When one phase (assuming the fifth phase) is open-circuited, the machine can still continue to operate using the four healthy phases. New current references are imposed in the four healthy phase in order to keep constant the generator torque.

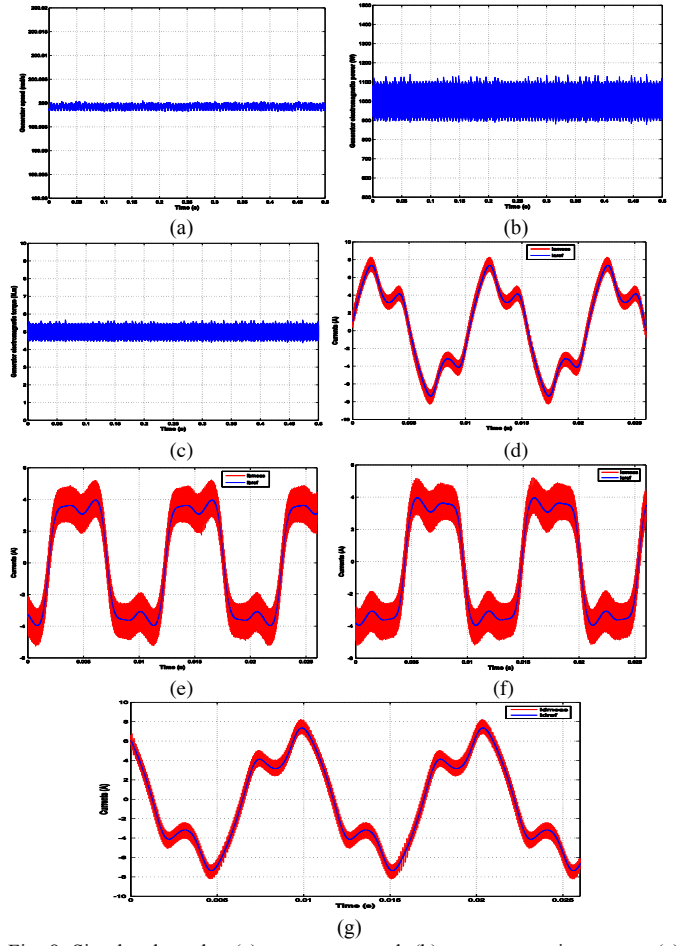
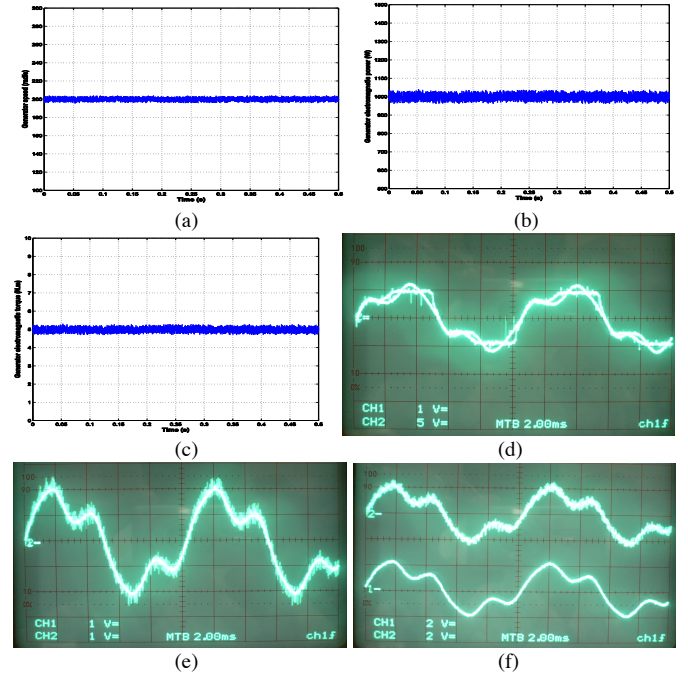


Fig. 8. Simulated results; (a) generator speed, (b) generator active power, (c) generator electromagnetic torque, (d) new currents in the phase a, (e) new currents in the phase b, (f) new currents in the phase c, (g) new currents in the phase d



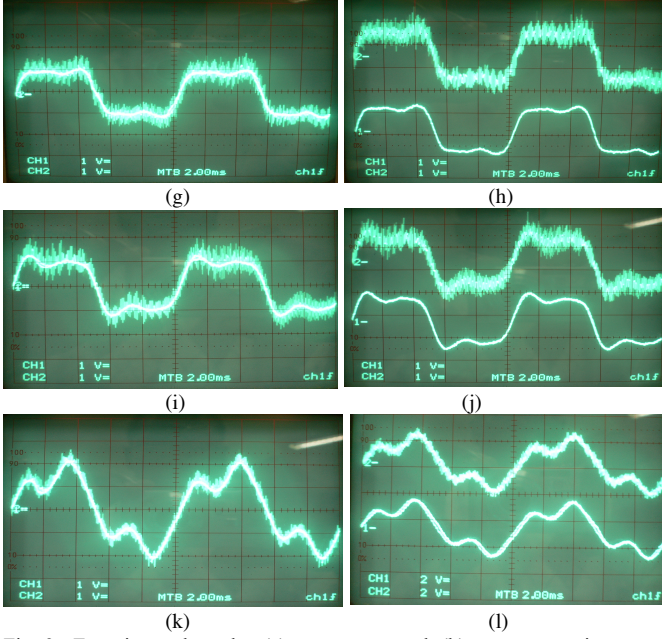


Fig. 9 . Experimental results; (a) generator speed, (b) generator active power, (c) generator electromagnetic torque, (d) I_a current reference and E_a EMF in the phase a, (e) and (f) new currents in the phase a, (g) and (h) new currents in the phase b, (i) and (j) new currents in the phase c, (k) and (l) new currents in the phase d

As it is normal operation, i.e. Figs. 8(d)(e)(f)(g), 9(e)(g)(i)(k) and 9(f)(h)(j)(l) show the good performance of the AC current controllers which accurately track their references. The phase shift between the new EMF (without load) and the current reference tends to zero as shown in Fig. 9(d). The generator torque is constant (Fig. 8(c), Fig. 9(c)) and there is no oscillation in the generator speed (Fig. 8(a), Fig. 9(a)) and the generator active power (Fig. 8(b), Fig. 9(b)). The numerical results torque ripples is given in TABLE III.

TABLE III
NUMERICAL RESULTS TORQUE RIPPLES

	Normal operation	fault operation	fault operation after corrections
Ratio between the torque ripples and the average value of the generator torque	0 % (see Fig. 6(d), Fig. 7(c))	60 % (see Fig. 3)	0 % (see Fig. 8(c), Fig. 9(c))

VII. CONCLUSION

In this paper an improved torque control strategy of five-phase PMSG-PWM rectifier is proposed for both normal operating mode and fault operating mode. Under normal operation a new vectorial modeling approach based on Fortescue's transformation is established. Under fault operation a new method based on the model of the five-phase PMSG - AC/DC rectifier set, to determinate the optimal current references, is developed. This method can be applied for any open phase. The adopted torque control strategy, for any operation, allows to reduce the torque ripples and to minimize the copper losses. The used controller ensures an effective tracking of the non-constants current references

imposed by the torque control strategy. Thanks to this controller, it is not necessary to know the model of the controlled system. Simulation and experimental results show the good performances achieved thanks to the AC current controller.

REFERENCES

- [1] E. Levi, "Multiphase electric machines for variable-speed applications," IEEE Trans. Ind. Electron., vol. 55, no. 5, pp. 1893–1909, May 2008.
- [2] T. M. Jahns, "Improved reliability in solid-state ac drives by means of multiple independent phase-drive units," IEEE Trans. Ind. Appl., pp. 321–331, May/Jun. 1980.
- [3] R. Fu and T. A. Lipo, "Disturbance-free operation of a multiphase current regulated motor drive with an opened phase," IEEE Trans. Ind. Appl., vol. 30, no. 5, pp. 1267–1274, Sep./Oct. 1994.
- [4] H. A. Toliyat, "Analysis and simulation of five-phase variable-speed induction motor drives under asymmetrical connections," IEEE Trans. Power Electron., vol. 13, no. 4, pp. 748–756, Jul. 1998.
- [5] N. Bianchi, S. Bolognani, and M. D. Pre, "Strategies for the fault-tolerant current control of a five-phase permanent-magnet motor," IEEE Trans. Ind. Appl., vol. 43, no. 4, pp. 960–970, Jul./Aug. 2007.
- [6] J. Wang, K. Atallah, and D. Howe, "Optimal torque control of fault tolerant permanent magnet brushless machines," IEEE Trans. Magn., vol. 39, no. 5, pp. 2962–2964, Sep. 2003.
- [7] Z. Sun, J. Wang, G. W. Jewell, and D. Howe, "Enhanced optimal torque control of fault-tolerant PM machine under flux-weakening operation," IEEE Trans. Ind. Electron., vol. 57, no. 1, pp. 344–353, Jan. 2010.
- [8] S. Dwari and L. Parsa, "An optimal control technique for multiphase PM machines under open-circuit faults," IEEE Trans. Ind. Electron., vol. 55, No. 5, pp. 1988–1995, May 2008.
- [9] F. Baudart, B. Dehez, F. Labrique, E. Matagne, "Optimal current waveforms for permanent magnet synchronous machines with any number of phases in open circuit" Mathematics and Computers in Simulation, Elsevier, Vol. 90, pp.1-14, April 2013.
- [10] X. Kestelyn and E. Semail, "A vectorial approach for generation of optimal current references for multiphase permanent-magnet synchronous machines in real time," IEEE Trans. Ind. Electron., vol. 58, No. 11, pp. 5057–5065, November 2011.
- [11] M. A. Fnaiech, F. Betin, G. A. Capolino, and F. Fnaiech, "Fuzzy logic and sliding-mode controls applied to six-phase induction machine with open phases," IEEE Trans. Ind. Electron., vol. 57, no. 1, pp. 354–364, Jan. 2010.
- [12] F. Mekri, S. Benelghali, M. E. H. Benbouzid, and J. F. Charpentier, "A Fault-tolerant multiphase permanent magnet generator for marine current turbine applications," in Proc. 2011 IEEE ISIE, Gdansk, Poland, Jun. 2011, pp. 2079–2084.
- [13] F. Mekri, S. Benelghali, and M. E. H. Benbouzid, "A Fault-tolerant control Performance comparison of three- and five-phase permanent magnet generator for marine current turbine applications," IEEE Transactions on sustainable energy, Vol.4, pp. 2079–2084, April 2013.
- [14] Hyung-Min Ryu, Ji-Woong Kim, and Seung-Ki Sul, "Synchronous Frame Current Control of Multi-Phase Synchronous Motor" Part II. Asymmetric Fault Condition due to Open Phases. IEEE Transactions on Industry Applications, Vol. 42, No. 4, pp. 1062-1066, July/August 2006.
- [15] A. Dieng, M.F. Benkhoris and M. Ait-Ahmed, "Torque Control Strategy of Non-sinusoidal Brushless DC Motor Based on Fractional Regulator". 21ST International Symposium on Power Electronics, Electrical Drives, Automation and Motion, Naples, Italy, pp. 207-212, June 2012.
- [16] A. Dieng, M.F. Benkhoris and M. Ait-Ahmed, "Torque Ripples Reduction of five phases PMSM using Fractional Order Regulator". XXth International Conference on Electrical Machines, ICEM, Marseille, France, pp. 1114-1120, September 2012.
- [17] B. Sari, A. Dieng, M.F. Benkhoris and M. Ait-Ahmed, "A new robust Torque Control of a five phases permanent magnet synchronous machine". 15th International Power Electronics and Motion Control Conference and Exposition, Novi Sad, Serbia, September, 2012.
- [18] Huangsheng Xu, H. A. Toliyat, and L. J. Petersen, "Resilient Current Control of Five-Phase Induction Motor under Asymmetrical Fault Conditions," Applied Power Electronics Conference and Exposition (APEC), pp.64-71, March 2002.

- [19] A.Dieng, J.C. Le Claire, M.F. Benkhoris and M. Ait-Ahmed. "Comparative evaluation of the Single-phase "VIENNA I" and the Double Boost Effect "DBE" rectifiers under sliding mode current control", Power Electronics and Applications (EPE), 2013 15th European Conference on, Lille, France, pp.1-10, September 2013.
- [20] J.C. Le Claire, S. Siala, J. Saillard, R. Le Doeuff, US patent n° 6.376.935 B1, April 23, 2002, "Method and device for controlling switches in a control system with variable structure, with controllable frequency.
- [21] J.C. Le Claire, Siala S., Saillard J., Le Doeuff R., "A new Pulse Modulation for Voltage Supply Inverter's Current Control", 8th European Conference on Power Electronics and Applications, Lausanne, Switzerland, September 1999, CD-ROM ref. ISBN 90-75815-04-2.
- [22] B. Whitby and C. E. Ugalde-Loo, "Performance of Pitch and Stall Regulated Tidal Stream Turbines" IEEE Transactions on Sustainable Energy, Manuscript received April 23, 2013 and accepted July 05, 2013 for inclusion in a future issue of this journal.
- [23] S. Benelghali and al., "Experimental validation of a marine current turbine simulator: Application to a PMSG-based system second-order sliding mode control," IEEE Trans. on Ind. Elec., pp 118-126, 2011.
- [24] C.L. Fortescue, "method of symmetrical coordinates applied to the solution of polyphase networks" Annual convention of the American Institute of Electrical Engineers, pp. 629-715, Junes 1918.
- [25] H. Sira-Ramirez, A. Luviano-Juarez, J. Cortés-Romero, "Robust input-output sliding mode control of the buck converter", Elsevier, Control Engineering Practice, March 31, 2012.
- [26] B. Putzeys, "Simple Self-Oscillating Class D Amplifier with Full Output Filter Control", 118th Convention of Audio Engineering Society AES, Barcelona, Spain, USA, May 28-31, 2005.
- [27] B. Putzeys, US patent n° 7.113.038 B2, PCT Filed, April 1, 2003, Date of Patent, September 26, 2006.
- [28] S.H. Lee, J.Y. Shin, H.Y. Lee, H.J. Park, "A 2W, 92% Efficiency and 0.01% THD+N Class-D Audio Power Amplifier for Mobile Applications, based on the Novel SCOM Architecture", in Proceedings of the 26th Custom Integrated Circuits Conference, Orlando, FL, USA, October 3-6, 2004, pp. 294-291.
- [29] I. Boiko, "Input-output analysis of limit cycling relay feedback control systems", in Proceedings of the American Control Conference, California, Jun 2-4, 1999.
- [30] J.C. Le Claire, E. Frappé, "Stability of a DC/AC converter involving a sliding mode voltage controller", EPE 2009, Barcelona, Spain, September 8-10, 2009.